Journal of Engineering Research

Volume 5 | Issue 4 Article 3

2021

Combustion performance of a two-layer porous inert medium burner at different low powers

Saeed Mahmoud Yahya, Ayman I. Bakry, Omar Abdelmotaal Mehrez

Vol. 5, No. 4 – 2021 Journal of Engineering Research (ERJ)

Combustion performance of a two-layer porous inert medium burner at different low powers

Saeed M. Yahya*, Ayman I. Bakry, Omar Mehrez

Department of Mechanical Power Engineering, Faculty of Engineering, Tanta University, Egypt.
Corresponding author email (saeed_yahya@f-eng.tanta.edu.eg)

Abstract- **Improving the performance of modern combustion systems in many engineering application fields has great favorable impact on the energy conservation and global environmental pollution. This can be done through developing state of the art techniques for this purpose. One of them is the combustion within porous media burners. The two-layer porous inert medium burner (PIM) has significant merits such as high burning ratios, very low emission levels, high levels of the combustion stability, and operation at ultra-lean excess air ratios. The main work is to examine a new PIM design has a square cross-section area with two porous layers namely, aluminum oxide as the subcritical layer (quenching layer) and silicon carbide (SiC) as the supercritical layer each of 130 x 130 mm. The burner performance was estimated by recording the axial temperature profile at the selected operated thermal powers. The extent of the combustion stability limits between the flashback limit to the blow-off limit was improved. The excess air ratios of the stability limits at powers 0.7, 1.5, 2.5 kW were deduced to be (1.9-2.8), (1.8-2.6), and (1.5-2.4), respectively. The exhaust emissions were measured by a gas analyzer. The results revealed low levels of the CO emissions and decreased with increasing the operated thermal power. The CO ppm recorded the order of hundreds at powers 0.7 and 1.5 kW but reached the order of tens at power 2.5 kW. The NOx emission recorded ultra-low levels and increase with increasing the thermal power but not exceed 2 ppm.**

Keywords: Porous inert media; aluminum oxide material; combustion stability; emissions levels

I. INTRODUCTION

The obstacles of depletion of fossil fuel resources coupled with the environmental pollution are due to the ever increase on energy demand and the rapid growth in the industrial field [1]. The improvement in the combustion process efficiency is one of the most promising solution to maintain the nonrenewable resources and minimize the environmental pollution [2]. Porous burner combustion is one of the most alternative solution for this purpose due to the remarkable characteristics which covers a wide range of practical applications [3]. The fascinating characteristics are including high thermal efficiency, low level of pollutant emissions, a wide range of lean flammability limits, high level of turn down ratio, enhancing the stability of combustion, the ability to operate in the ultra-lean combustion regimes, and high burning rates as compared to conventional combustion [4-7].

Numerous efforts have been made to improve alternative combustion techniques. They seek to achieve two important key features in the development of Porous Inert Medium (PIM) combustion technique [6, 8]. The first approach is the theory of excess enthalpy, which represents how the three heat transfer modes interact between the gas and solid phases [9]. The most significant key feature is the effective preheating of incoming reactants. The released thermal energy is internally recirculated from the hot gases produced in the reaction zone returning to the incoming cold reactants without direct contact [10]. Many researchers exhibit the effect of excess enthalpy to enhance the self-sustaining combustion wave through the imposed super adiabatic combustion condition, the flammability limits extension to the compositions of the very diluted mixtures, and the burning speed, where this theory is most relevant and beneficial to the present work [9, 11, 12].

The second approach is mainly specifying all possible regimes at the ambient conditions, which occurs through the PIM materials during the propagation of the combustion wave. The high and low velocity regimes are considered as the most important regimes to describe the combustion wave propagation in the PIM burner [13]. The operation of PIM burners is categorized basically into two modes namely submerged (or matrix) and surface stabilized combustion [6]. The combustion of fuel in the first mode occurs in the pores of the porous media, where a direct combustion of the unreacted fuel occurs on or above the radiating surface of the medium. Surface stabilized combustion mode has distinctive characteristics as the combustion occurs just above the porous surface, where the hot gases above the porous surface heats the radiating surface. This type of burner is widely used commercially and industrially [14].

A dimensionless critical and crucial criterion was created by modifying the form of Peclet number [13, 15-17]. It was used to measure where the combustion wave would propagate in which of the two of high-low velocity regimes. Physically, Peclet number was defined as the ratio between the total thermal energy produced from the combustion process to the total energy lost into the solid material of PIM burner. Mathematically, it was defined as ($Pe = S_l . d_{p,eqv}/ \alpha_m$), where the parameters S_l , $d_{p,eqv}$, α_m indicated to the laminar burning velocity , the equivalent pore diameter of the porous material, and the thermal diffusivity of the unburned reactant mixture, respectively. The critical value of Pe was 65, this value represented the base of the stability of combustion within all PIM techniques. It was shown that the only independent parameter that controlled the Peclet number criterion was the equivalent pore diameter ($d_{p,eqv}$) at a specific reactant composition and operating conditions for a constant PIM material. However, the remain parameters only were affected by the initial and operating conditions. The super-critical combustion mode occurred at $Pe > 65$, where the combustion wave was propagating in the high-velocity regime. In contrast, at $Pe < 65$ the subcritical combustion mode occurred with the

propagation or quenching of the combustion wave in the low-velocity regime [13, 18]. It was observed that the incoming reactants propagates in the opposite direction of the combustion wave, whereas the combustion wave was held stationary or propagated in both directions in the subcritical mode [19, 20]. Also, the preheating degree of the PIM materials and the flow velocity of the reactants (filtration velocity) had the most significant effect on the combustion wave in the subcritical mode [18].

The stabilization of the combustion wave in a two-layer of PIM materials can be achieved by using different pore size materials. The upstream layer (quenching layer) has a pore size diameter less than the critical value, which satisfy the mode of the subcritical combustion [21]. The pore size diameter of the downstream layer is higher than the critical value to reach the supercritical operating mode. As a result, at the moment of ignition at its downstream surface, the combustion wave spreads out in the upstream direction toward the interface surface [21, 22]. The two-critical blow-off and flashback limits are considered the basic limits which determine the stability range of combustion within the two-layer PIM technique. It is noted that the blow-off critical condition occurs when the air to fuel ratio increases a critical value. For this specific case, the physical effects of the convection heat transfer at the interface and the supercritical layer overcome such effects of the conduction and the radiation heat transfer [15, 18]. The combustion wave moves in the direction of the downstream surface exceeding the interface surface and a blue and small flame begins to appear. In contrast, the critical flashback condition occurs instantly when decreasing the air to fuel ratio to a limiting value. The radiation and the conduction effects become stronger while the convection effects in the subcritical layer diminish. The previous phenomena occur due to the lean mixture and the high temperature in the downstream surface of the supercritical layer [23-26].

The technique of the two-layer (quenching or preheating and combustion layers) PIM burner was studied from many researchers since the last few decades [22, 27-29]. They studied the variation of many parameters on the performance, the stability range, the thermal efficiency, and the emission ratios of the PIM burner. The characteristics of the combustion stability of PIM was improved by Bakry [5] by using a modified technique of the quenching layer concept. The burner was made of cylindrical shape and had two main parts. The lower part (quenching layer) includes 19 mm slotted firebrick layer, a steel disc of 110 mm diameter and 1.6 mm thickness was slotted at the same panner as the brick layer, and a steel ring of 110 mm diameter, 9 mm height, and 0.6 mm thickness. However, the upper surface consists of wire mesh made of nickel-chromium alloy with dimensions of 130 mm height and 85 mm diameter. It was proved that the burner could operate under wider stable ranges of fuel-lean mixture. Also, over all these entire ranges, the flashback condition was observed to be eliminated. In addition, CO and NOx were very low [5].

Bakry et al. [4], also studied the performance and the stability limits of a rectangular design mainly consisted of a preheating plate of Cordierite material with dimensions 130 x 130 mm square section and 13 mm thickness. The reaction zone was an exchange between two different materials of SiC foam (10 ppi & ~87% porosity) and a wire mesh of Nickel-chromium steel alloy (> 95% porosity). The burner was operating at low thermal powers (0.7-2.5 kW). They studied the conditions of the unsteady flashback, stable, and the unsteady blow-off to determine the stability limits diagram. During operating at the thermal power of 1.5 kW, the peak excess air ratios of flashback and blow-off limits occurred at 2.2 and 2.8, respectively. The common stability ratios 2.2-2.4 are recommended. They obtained ultra-low NOx-emissions (< 2 ppm), but obviously, the CO-emissions were high at powers ≤ 1.5 kW.

Janvekar et al. [30] studied the effect of using different thicknesses of the porcelain foam preheat layer on the surface and submerged flame. The thicknesses were 5, 10, and 15 mm. The surface flame was only visible when using 5 mm preheat layer, while the surface and the submerged flame could occur when using 10 and 15 mm preheat layer. The best performance was observed at equivalence ratio 0.7 and 0.5 for the surface and submerged flame, respectively. According to the thermal efficiency, it reached its highest value 90% for the surface flame and 38% for the submerged flame at the 10 mm preheat layer. The NOx and CO emissions were recorded lower rates for all case.

Most reviewers exhibited different designs of the PIM burner and perfectly expressed its combustion performance. The current study would provide a new modified PIM burner design with a new material type of the subcritical layer. The combustion stability limits and the emissions levels were accurately experimented and recorded and as a result, the burner performance could be exactly estimated.

II. Experimental Setup and Procedure.

The main features of the PIM burner in the present study are schematically demonstrated in figure 1 including the burner system with a mixing section, the control devices, and the measurement instruments. The required air is supplied from a compressor with 500-liter capacity and 7.5 horsepower. The desired air flowrate is firstly filtered and can be adjusted by a fine needle valve and measured by an accurate mass flow meter (Omega FMA-A2323). It has a range 0-100 SLM and an accuracy of ±1% of the full scale. The filtered air is regulated to be constant at 2 bars using a pressure regulator and delivered to the mixing section with the LPG gaseous fuel. The fuel flow rate is measured by a mass flow meter (Omega FMA-A2313). Its range and accuracy are 0-30 SLM and ±1% respectively and is also adjusted by a fine needle valve. The standard volumetric concentrations, density, and lower calorific value of the LPG fuel were 1.3% C2H6, 19.9% C3H8, 28.5% ISO−C4H10, 47.3% C4H10, 2.1% ISO−C5H12, 0.9% C5H12, 2.3436 kg/m3, and 106.676 kJ/m^3, respectively. The air and the fuel are well mixed through the mixing section. The air-fuel mixture is delivered to a square settling chamber at the base burner within a U-shaped tube of 25.4 mm in diameter. The mixture is uniformly distributed as a result of passing through a square and porous insulating material with dimensions 130x130x13 mm and porosity ~90%. It is also used to protect the burner system from the dangerous

flashback conditions by quenching the backfire. Then, the mixture is directed to the upstream surface of the porous quenching material (Pe < 65) which is made of aluminum oxide (80% Al2O3+19.5% SiO2) with dimensions 130x130x13 mm. it has 1mm hole diameter and porosity~ 11.8% and can be operated under 1600°c. The other layer which is called the supercritical layer and is in good contact on the downstream surface of the preheating layer. It is made of silicon carbide (SiC) and has a porosity ~80%. Its dimensions are 120x120x40 mm and Pe > 65. The upper part of the burner is as a chimney to eject the exhaust gases produced from the combustion process occurred at combustion layer. A sample of the exhaust gases can be extracted by the probe of a gas analyzer (Testo 340) at a location of 250mm from the reference point at the upper part of the burner as shown in figure. 1. The CO, NOx, and O2 concentrations can be measured simultaneously through the gas analyzer which has ranges for the CO, NOx, and O2 as 0-10000 ppm, 0-3000 ppm, 0-25% with resolutions of 1 ppm, 1 ppm, and 0.01% and accuracies ± 10 ppm (0-200 ppm), ± 5 ppm (0-99 ppm), and ± 0.2 vol%, respectively. According to the value of the O2 concentration, the CO2 concentration can be calculated internally through the gas analyzer. Also, the O2 concentration value compared with the excess air ratio which is adapted from the two flowmeters mentioned before. 2.1% is the maximum difference between the two methods. All parts of the burner body are made of a thin sheet metal of 2mm thickness. The burner walls are thermally insulated at the inner side.

There are seven thermocouples axially installed along the burner in order to analyze the temperature distribution produced from the combustion process. The interface surface between the preheating and the quenching layers is taken to be the reference position (zero gauge) where the thermocouple T_3 is installed as shown in figure 1. The thermocouple T_4 is installed at +40 mm at good contact to the downstream surface of the SiC material. The two thermocouples T_3 and T_4 are used to determine where the fire will stabilize. The first two thermocouples T_1 and T_2 are installed under the zero gauge at locations -13 mm and -100 mm, respectively. Both are used to detect the creation of the unstable flashback condition. All the prementioned positions are not standard positions, but they are personally chosen to completely explain the temperature profile along the whole burner. The type of the T_3 and T_4 thermocouples are S-type but the remaining thermocouples are K-type. All of them are connected to OM-DAQXL (Multi-Channel Universal Input Touch Screen Data Logger) which displays and records the temperature readings simultaneously at a rate of 1 sample per second (samp/sec). Each type of the K and S-types are adapted from the data logger with accuracy of ± (0.15% of reading + 1.1 °C) and ± (0.15% of reading + 2.0 °C), respectively. The average time constant of the K and S-types was calculated experimentally and was about ~ 0.35 s and ~ 0.3 s, respectively.

Before starting up the experiment, the required value of the LPG flow rate can be adjusted within the LPG mass flow meter to satisfy the designated thermal power. After that, the corresponding excess air value is adjusted through the air mass flow meter. The combustion starts after igniting the top surface of combustion layer and it is left developing for about 10 minutes. The temperature distribution is recorded each one second for a long period, minimum one hour, to examine the performance of the combustion stability. The limits of the unstable flashback and blowoff conditions are determined by increasing the excess air ratio of 0.1 for each constant thermal power. The emissions of the combustion gases are measured at constant periods. However, they are recorded for only the stable cases. All the experimental runs are conducted at ambient pressure and temperature which is varied from 25 °C and 33 °C.

The operating parameters of the burner could cause some uncertainties in the experimental results. Uncertainties analyses would be important to validate the accuracy of the experimental results. According to the technique of Moffat [31], the uncertainties analyses for the LPG properties and the burner parameters were made. Such properties were the LPG calorific value, the LPG density, the excess air ratio, and the thermal power. The relative errors percentages of the previous properties were 1.20%, 1.22%, 1.87%, and 1.98%, respectively. A real photo of the PIM burner setup in the lab was demonstrated in figure 2.

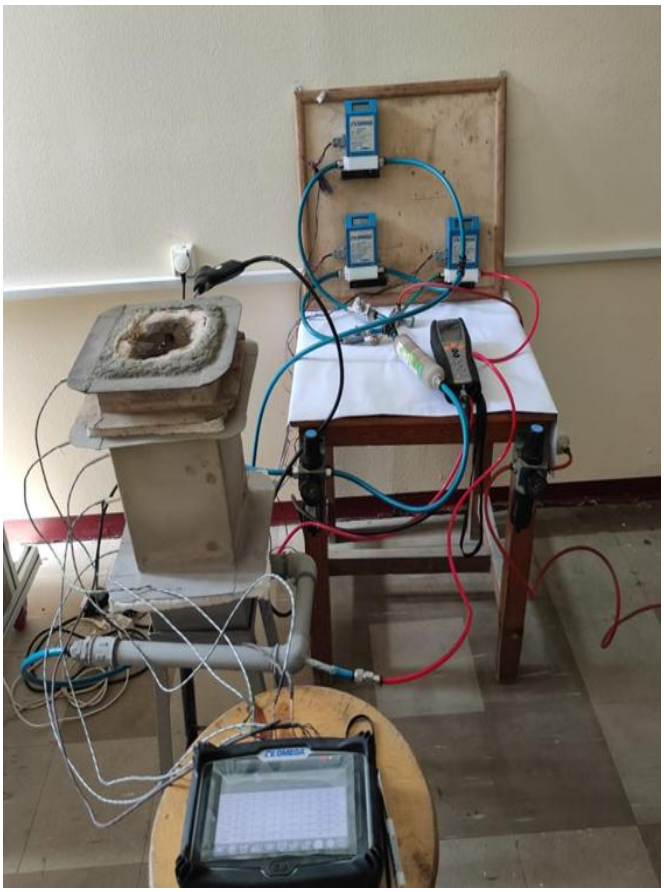

Fig. 1: A real photo of the experimental setup in the lap.

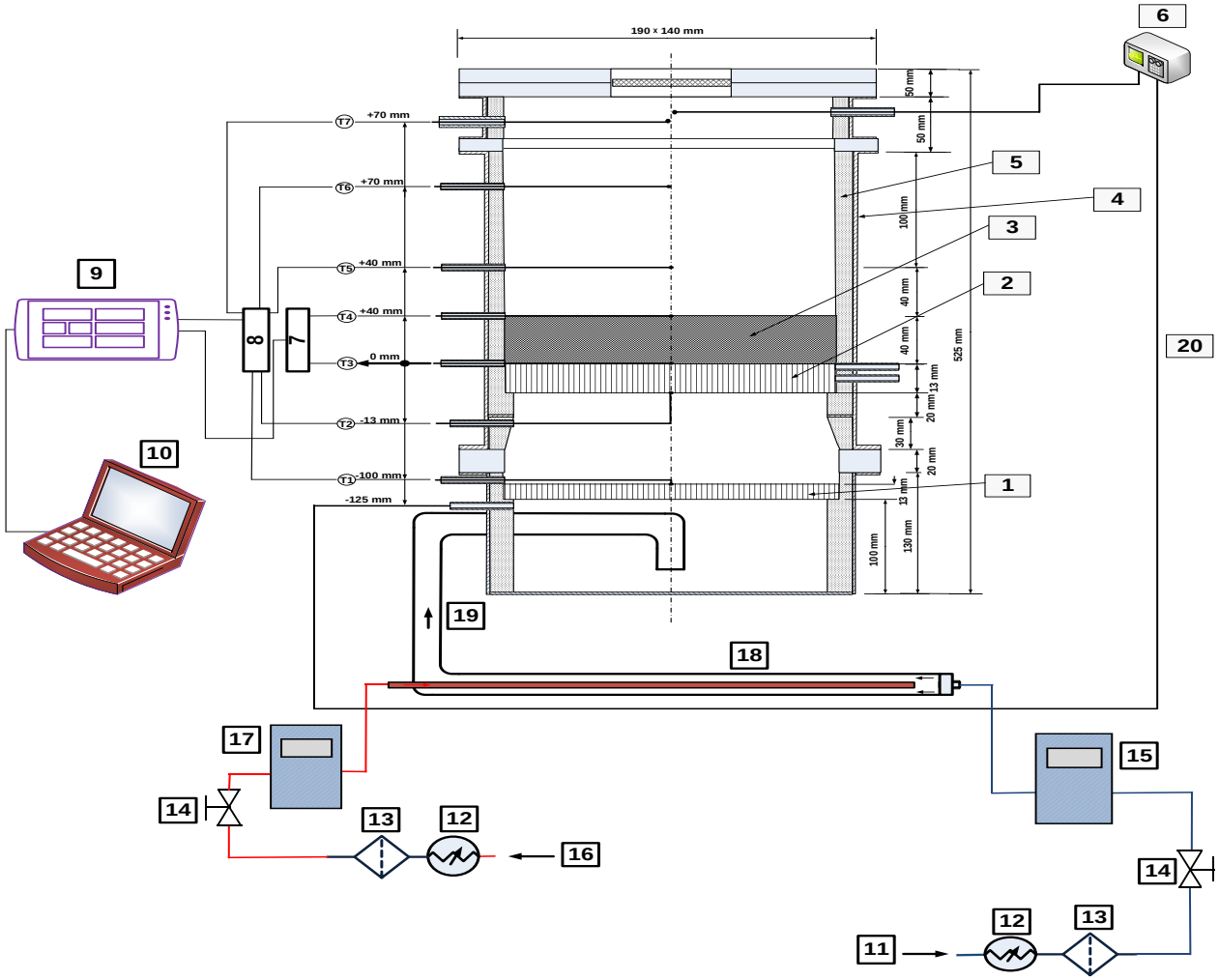

1	Porous Insulating Material	9	Data Logger	17	Gas Mass Flow Mete
2	Subcritical Quenching Layer	10	Laptop	18	Mixing Section
3	Supercritical Combustion Layer	11	Compressor Line	19	LPG & air mixture
4	2 mm Steel Body	12	Pressure Regulator		
5	Thermal Insulation Material	13	Air Filter		
6	Gas Analyzer	14	Needle Valve	20	Pressure Drop Measuring Line
7	S-type Thermocouples	15	Air Mass Flow Meter		
8	K-type Thermocouples	16	LPG Gas Bottle		

Fig. 2: Schematic drawing of the burner setup in details and the measuring instruments.

III. RESULTS AND DISCUSSIONS

A. Temperature distributions at various times and the combustion stability limits

The temperature distribution along the burner axis were recorded within seven thermocouples along the axial arrangement. The main study was to deduce the effect of using a new burner design with a new type of the preheating material made of (80% Al2O3+19.5% SiO2) on the combustion stability limits and the burner emissions. As shown in figures 3-7, the burner had been examined at three different thermal powers 0.7 kW, 1.5 kW, and 2.5 kW. In order to clarify all conditions of the combustion stability limits, the operational experiments had been done at various excess air ratios from the unstable flashback to the unstable blow-off limits including the stable conditions with an increment of 0.1 for each value of the excess air ratio. For each thermal power, there were five excess air values were chosen to represent all the stable and the unstable cases, namely: the unstable flashback limit, the stable flashback value just above its unstable limit, the perfect stable condition between the two limits, the stable blow-off value just before its unstable limit, and the unstable blow-off limit. All the previous conditions were studied at the prementioned three thermal powers. It is worth noting that all the stable experiments had been occurred for about at least one hour or longer according to each case. Before start recording the temperature readings, the burner had been left getting warm for about 10 minutes at a certain excess air value at t = 0 which guaranties a secure stable combustion. Also, the real time of the other unstable states

were recorded after readjusting the special secure moment at t = 0 and the behavior of the unstable states could be studied.

As shown in figure 3, the constitution of the unstable flash back condition could be observed by the first two thermocouples T_1 and T_2 where $T_2 > T_1$. It was noticed that the temperature values of T_2 and T_1 rise slowly due to the slow

the reactant of mixture starts within the space between the quenching layer and the insulating layer. This is called the unstable flashback and can be observed from the rapid jump of the values of T_2 and T_1 with an interval of 1 s as they are presented by various red lines. It was also observed that the temperature at the interface between the two porous layers was slightly decreasing with time due to the heat loss during the propagation of the combustion wave through the upstream direction. This behavior of the unstable flashback approximately occurs for all the thermal powers. Evidently, the value of the excess air ratio of the flashback condition decreases with increasing the operated thermal power.

According to figure 7, the unstable blow-off condition was creating at relatively higher excess air ratios and could be detected by observing the temperature readings of T_3 and T_4. It was obvious that the temperature value of T_3 decreasing with time but the values of T_4 increasing. The combustion wave spreads moving towards the downstream direction until getting out from the SiC layer to the exit plane which the combustion flame is blue. The value of T_3 is still reducing until reaching at a value between 100 and 150 °C, so the blow-off condition is observed to be terminated. The results showed that the unstable blow-off condition exhibits the same trend of the unstable flashback condition with respect to the increasing of the operated thermal power.

The other values of the excess air ratios between the unstable values at the flashback and the blow-off conditions expressed the range of the stable conditions including the stable flashback, perfect stable, and the stable blow-off conditions. These conditions were observed from the temperature readings of T_2, T_3, and T_4. As exhibited in figures 4, during the stable flashback condition, the combustion wave was moving toward the upstream direction until is stabilized at a point within the subcritical layer due to the thermal balance among all modes of heat transfer. That behavior was observed during the gradually raising of the T_2 and T_1 values until they became constant. On the other hand, as presented in figure 6, the combustion wave during the stable blow-off condition was moving toward the downstream surface until it stabilized at a point within the supercritical layer also due to the heat balance. During that behavior, the T_3 value was gradually decreasing, but the T_4 value was gradually increasing until both became constant. Figure 5 explained the perfect stable condition occurred when the combustion wave stabilized at the interface surface between the two layers. The temperature reading of T_3 recorded its peak value during that perfect condition and the values of T_3 and T_4 remains constant along the operating time. The perfect stable condition is the best recommended condition to the PIM users as it gives the best performance of the combustion process and the PIM burner in general. All stable cases were presented in figures 4-6 for all operated thermal powers.

propagation of the combustion wave toward the upstream direction at the relatively low thermal powers. However, at high thermal powers the values of T_2 and T_1 rise faster. After reaching the ignition temperature value at the upstream surface of the quenching layer, the combustion of

Figure 8 presented the final results of the stability limits of the combustion within the PIM burner for all the different three thermal powers. The curves were plotted between the excess air ratios versus the corresponding thermal powers. Again, the results exhibited an obvious trend that the limits values of the excess air ratios decreasing to values close to the stoichiometric value when the thermal power was increasing, so the lowest values of the unstable blow-off and flashback limits occurred generally at the applied thermal power 2.5 kW. These results are very important for the PIM designers to use the suitable power according to each application. Generally, it was deduced that the combustion performance and the combustion stability limits within the porous media were improved for this new design and the new quenching material comparing with the other published research.

B. Emission analyses for the stable combustion cases.

The emissions ratios produced during the combustion through the PIM burner could be taken as an indication of the burner performance. The CO emissions were relatively observed for all the stable combustion cases, so they were the study of interest. The formation of the CO emissions was previously expected as the burner was mostly operating under highly diluted excess air ratios for most of the studied powers except the relatively high powers. The CO emissions were measured and recorded each 10 minutes along the operating time of the stable experiment to check the recorded value. Figure 9 showed the ppm values of the CO emissions with various excess air ratios for all the three studied powers presented for each thickness. It was observed that the CO emission level decreased with increasing the operating thermal power. The CO levels were relatively higher when operating at 0.7&1.5 kW thermal powers where the readings reached the order of hundreds of the ppm. The ppm values reduced to the order of tens at 2.5 kW. The previous results were expected due to the higher temperature profiles which occurred when operating at relatively high powers. Those reliable conditions were enough to oxidize the produced CO ppm into CO2. It was obvious that the CO levels recorded its maximum value at 0.7&1.5 kW thermal powers specially when operating at the excess air ratios of the stable flashback and blow-off conditions for all the operated thermal powers. That phenomenon occurred due to the random behavior of the condition that happened just before the unstable conditions of the flashback or the blow-off conditions. Figure 9 showed one minimum value of the CO emission for each curve. The minimum values for the three curves all were occurred at the perfect stable condition for each particular thermal power which is the best preferred operated condition that produced the highest combustion temperature with a perfect distributed combustion and in turn the CO emission reduced. As deduced before, when the operated thermal power increased, the

stability curve was moved towards the stoichiometric value and in turn the minimum CO value was moved

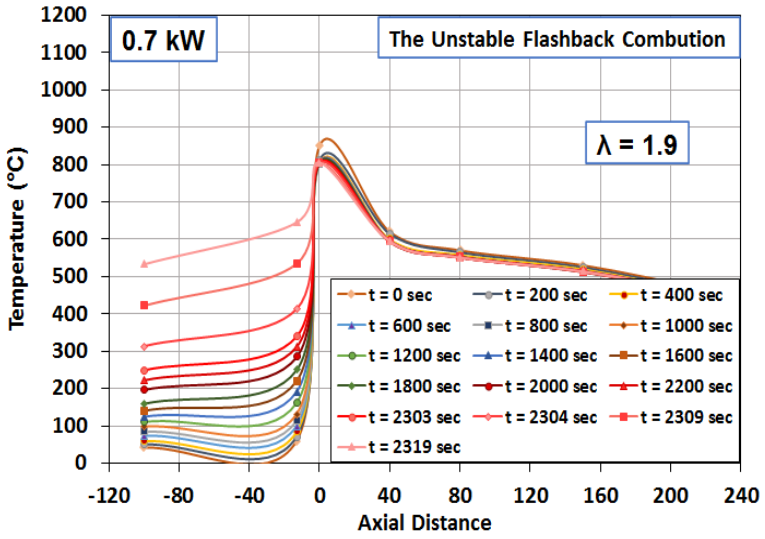

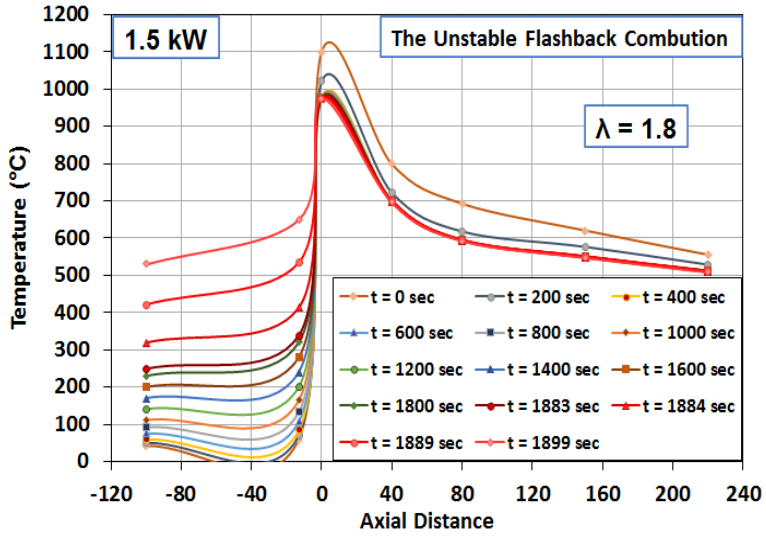

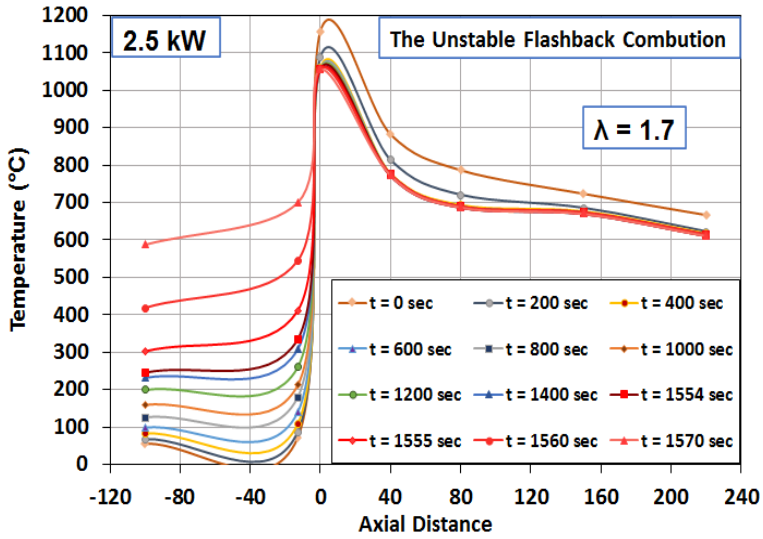

Fig. 3: Axial temperature distribution profile of the unstable flashback condition through the entire PIM burner at three thermal powers of 0.7, 1.5, and 2.5.

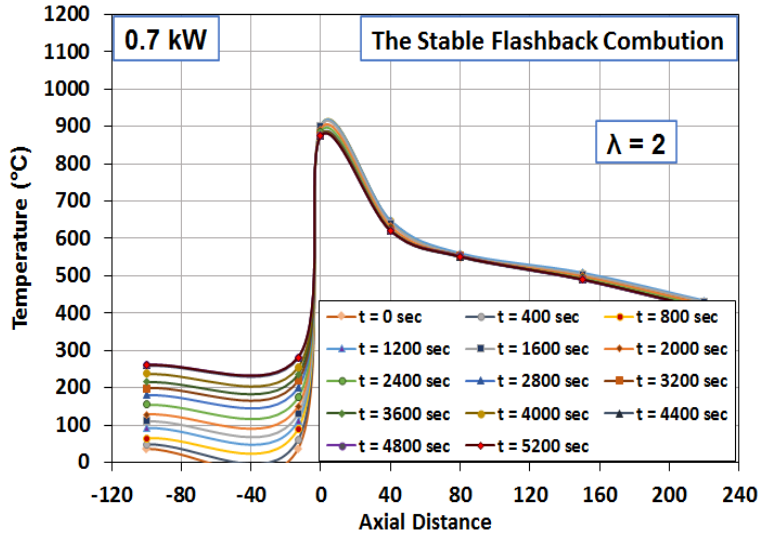

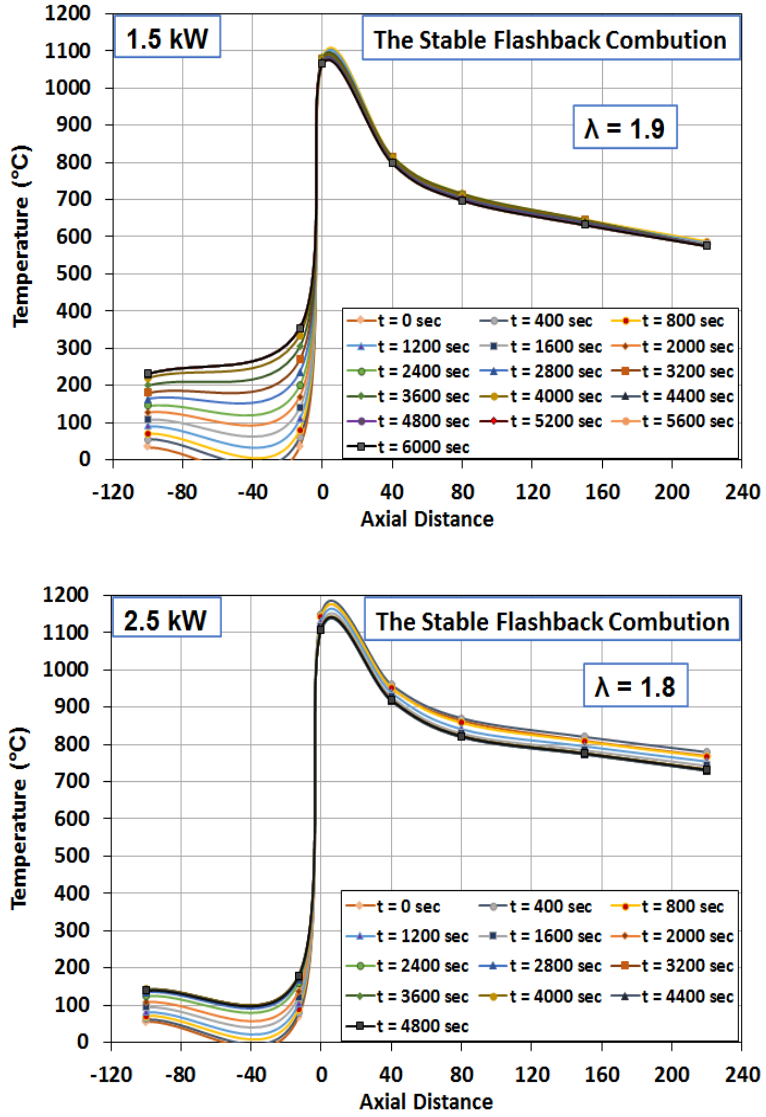

Fig. 4: Axial temperature distribution profile of the stable flashback condition through the entire PIM burner at three thermal powers of 0.7, 1.5, and 2.5 kW.

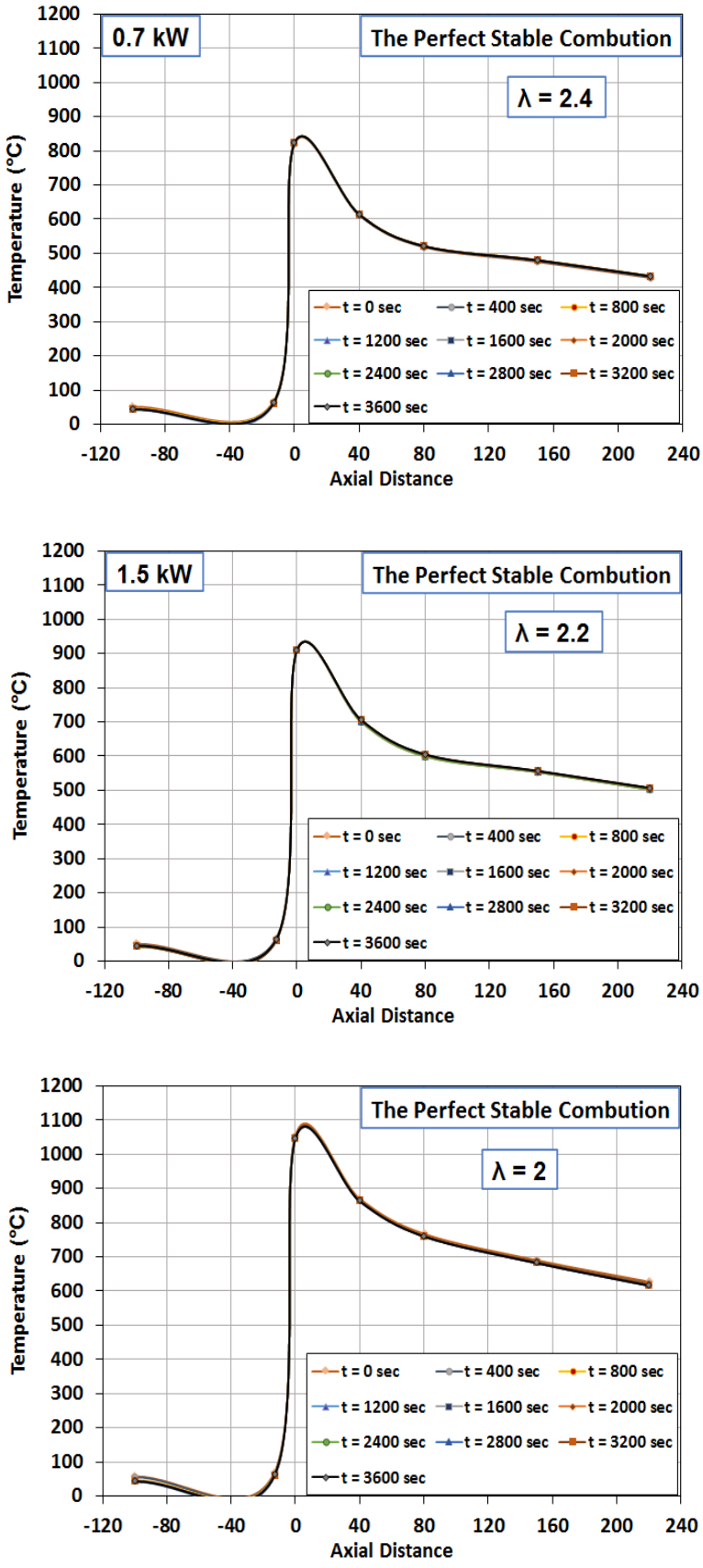

Fig. 5: Axial temperature distribution profile of the perfect stable condition through the entire PIM burner at three thermal powers of 0.7, 1.5, and 2.5 kW.

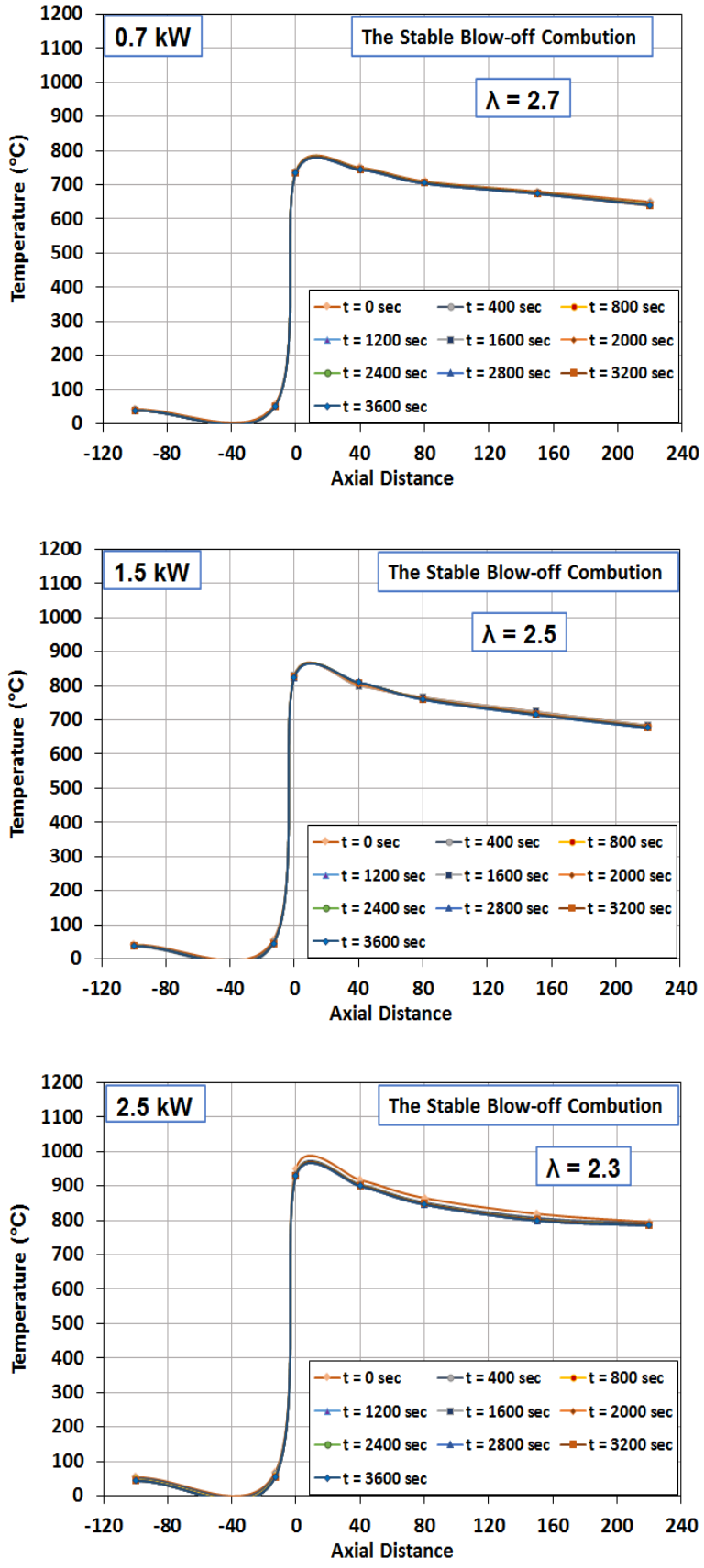

Fig. 6: Axial temperature distribution profile of the stable blow-off condition through the entire PIM burner at three thermal powers of 0.7, 1.5, and 2.5 kW.

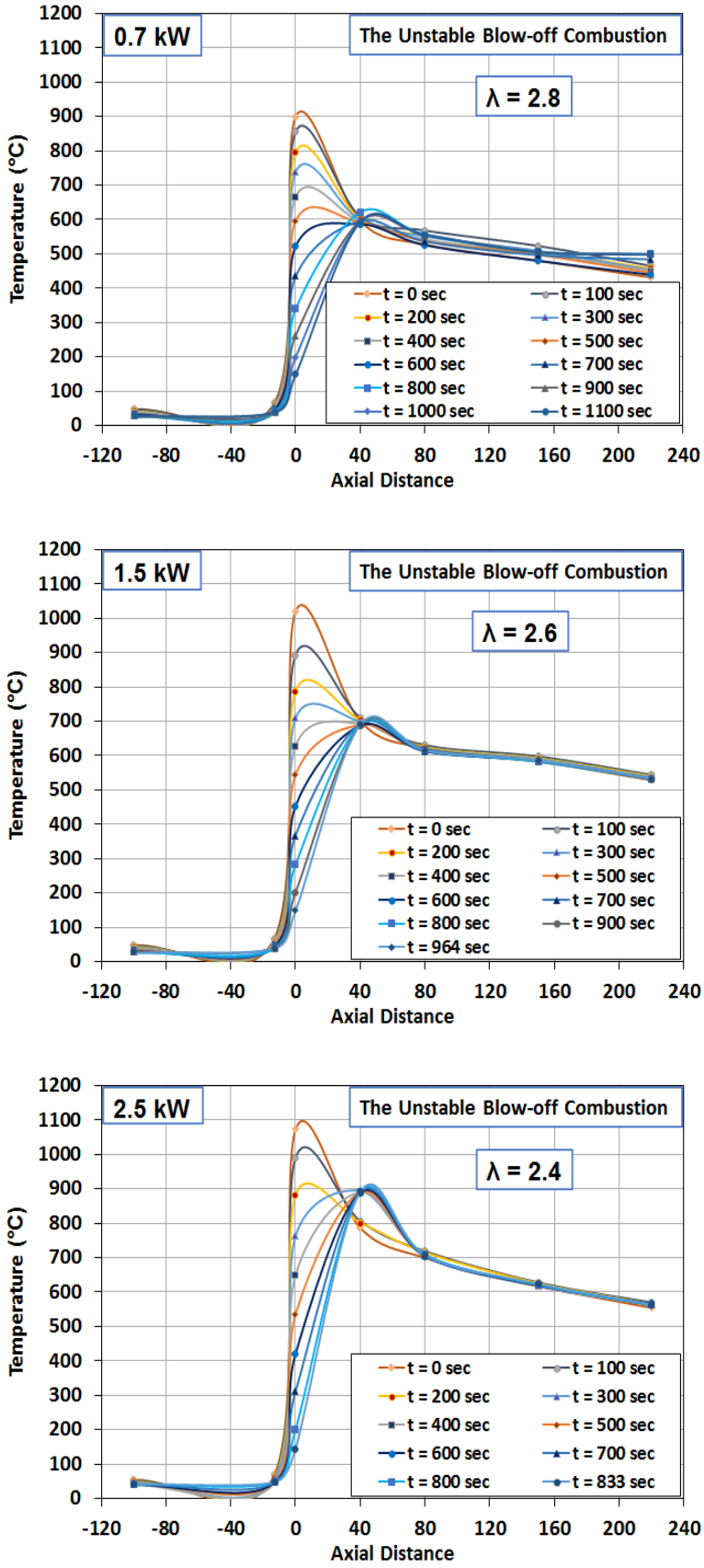

Fig. 7: Axial temperature distribution profile of the unstable blow-off condition through the entire PIM burner at three thermal powers of 0.7, 1.5, and 2.5

The emissions of NOx were also measured for all operated thermal powers and excess air ratios which experimented for this study using the Testo 340 gas analyzer. The experiments showed ultra-low levels of NOx emissions (< 2 ppm) and sometimes vanished specially when operating at 0.7&1.5 kW due to the reduction of the combustion temperature and the other circumstances that were needed to produce the NOx exhaust. However, about 1 or 2 ppm of NOx obtained when operating at 2.5 kW thermal power due to the relatively operating high combustion temperature.

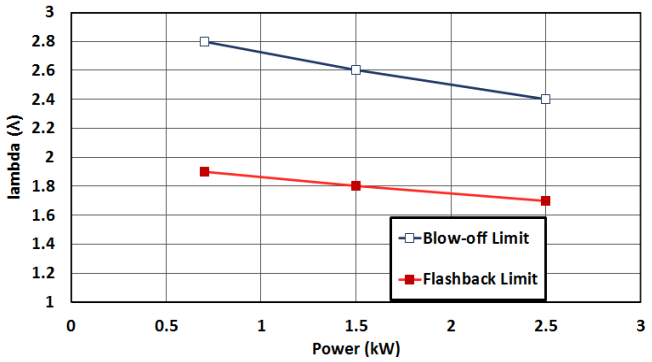

Fig. 8: The range of the combustion stability limits within a two-layer PIM burner operating at three different thermal powers 0.7, 1.5, and 2.5 kW.

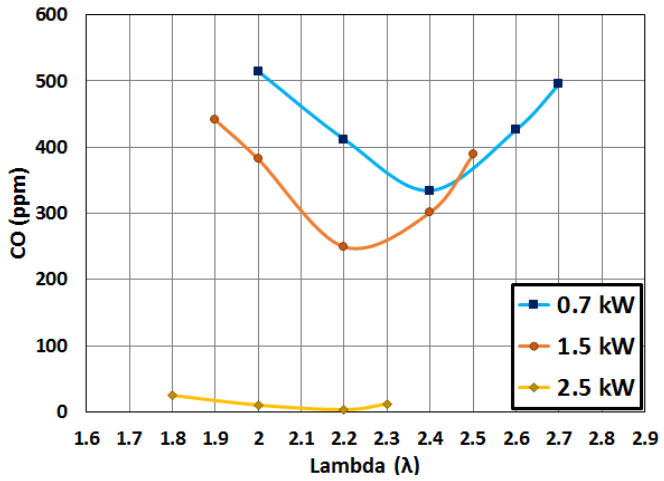

Fig. 9: The analysis of the CO-emissions of the combustion within a two-layer PIM burner operating at different three thermal powers 0.7, 1.5, 2.5 kW.

IV. CONCLUSION

This study was made to clarify the performance of a new PIM burner using a new subcritical material including the combustion stability limits and the resulting emissions. This was accomplished after operating at various thermal powers 0.7, 1.5, and 2.5 kW and recording the temperature profile axially along the hole burner and the emissions as well. New outcomes and phenomena were extracted from this study and can be briefly summarized in the following:

- Using a new material of the quenching layer, it was noticed an obvious difference on the stability limits compared with the published data that used other appropriate materials that have the same dimensions and porosity.
- The range of the stability limits shrank continuously with increasing the operated thermal power. The range between the flashback and the blow-off limits when operating at 0.7, 1.5-, and 2.5-kW thermal powers were (1.9-2.8), (1.8-2.6), and (1.7-2.4) respectively.
- For this special material of the quenching layer, the results showed that the stability limits trend close to the stochiometric excess air ratio with increasing the operating thermal power.
- The exhaust CO emissions were noticed to be at very low levels at 2.5 kW thermal power (≤25 ppm), at moderate levels at 1.5 kW (≤ 440 ppm), and at relatively high levels at 0.7 kW (≤515 ppm). The CO emissions were basically independent on the excess air ratios and the material types of the PIM layers.
- The CO emissions recorded its minimum value at the perfect stable condition for all the operated thermal powers.
- The exhaust NOx emissions recorded ultra-low levels (≤ 2 ppm) over the entire range of the excess air ratios and the operating thermal powers.
- The preheat layer type proved that it has a radical effect on the porous media burners, so it is recommended for researchers to design new techniques for studying all parameters of the preheat layer to achieve the optimum operated performance of that branch of burners.
- It is also recommended to use more advanced devices like thermal cameras to accurately measure the axially temperature distribution along the burner and the exhaust emissions, so the burner performance could be perfectly estimated.

REFERENCES

[1]. Muthukumar, P., and P. I. Shyamkumar. "Development of novel porous radiant burners for LPG cooking applications." Fuel 112 (2013): 562-566.
[2]. Khalil, A., et al. "Experimental study of cotton stalks gasification in a downdraft reactor." Journal of Engineering Research 2.August (2018): 1-15.
[3]. Keramiotis, Christos, and Maria A. Founti. "An experimental investigation of stability and operation of a biogas fueled porous burner." Fuel 103 (2013): 278-284..
[4]. Bakry, Ayman I., et al. "Performance of two-region porous inert medium burners operating at low thermal powers." Applied Thermal Engineering 141 (2018): 200-214..
[5]. Bakry, A. I. "Stabilized premixed combustion within atmospheric gas porous inert medium (PIM) burner." Proceedings of the Institution of Mechanical Engineers, Part A: Journal of Power and Energy 222.8 (2008): 781-789.
[6]. Mujeebu, M. Abdul, M. Z. Abdullah, and A. A. Mohamad. "Development of energy efficient porous medium burners on surface and submerged combustion modes." Energy 36.8 (2011): 5132-5139.
[7]. Trimis, Dimosthenis. "Stabilized combustion in porous media-applications of the porous burner technology in energy-and heat-engineering." Fluids 2000 conference and exhibit. 2000.
[8]. Dai, Hongchao, et al. "Combustion characteristics of a low calorific gas burner with ceramic foam enclosed by alumina pellets." Heat and Mass Transfer (2021): 1-11.
[9]. Takeno, Tadao, and Kenji Sato. "An excess enthalpy flame theory." Combustion Science and Technology 20.1-2 (1979): 73-84.
[10]. Lieuwen, Tim, et al. "Fuel flexibility influences on premixed combustor blowout, flashback, autoignition, and stability." Journal of engineering for gas turbines and power 130.1 (2008).
[11]. Barra, Amanda J., and Janet L. Ellzey. "Heat recirculation and heat transfer in porous burners." Combustion and flame 137.1-2 (2004): 230-241.

[12]. Colorado, A., and V. McDonell. "Surface stabilized combustion technology: An experimental evaluation of the extent of its fuel-flexibility and pollutant emissions using low and high calorific value fuels." Applied Thermal Engineering 136 (2018): 206-218.
[13]. Babkin, V. S., A. A. Korzhavin, and V. A. Bunev. "Propagation of premixed gaseous explosion flames in porous media." Combustion and Flame 87.2 (1991): 182-190.
[14]. Kamal, M. M., and A. A. Mohamad. "Combustion in porous media." Proceedings of the Institution of Mechanical Engineers, Part A: Journal of Power and Energy 220.5 (2006): 487-508.
[15]. Pan, H. L., O. Pickena¨ cker, and D. Trimis. "Characterization of pore diameters in highly porous media." Heat Transfer Summer Conference. Vol. 36940. 2003.
[16]. Trimis, Dimosthenis, and Klemens Wawrzinek. "Flame stabilization of highly diffusive gas mixtures in porous inert media." J Comput Appl Mech 5.2 (2004): 367-381.
[17]. Bubnovich, V., et al. "Experimental investigation of flame stability in the premixed propane-air combustion in two-section porous media burner." Fuel 291 (2021): 120117.
[18]. Ciccarelli, G. "Explosion propagation in inert porous media." Philosophical Transactions of the Royal Society A: Mathematical, Physical and Engineering Sciences 370.1960 (2012): 647-667.
[19]. Bakry, Ayman, et al. "Adiabatic premixed combustion in a gaseous fuel porous inert media under high pressure and temperature: Novel flame stabilization technique." Fuel 90.2 (2011): 647-658.
[20]. Wood, Susie, and Andrew T. Harris. "Porous burners for lean-burn applications." Progress in energy and combustion science 34.5 (2008): 667-684.
[21]. Trimis, D., and F. Durst. "Combustion in a porous medium-advances and applications." Combustion science and technology 121.1-6 (1996): 153-168.
[22]. Mujeebu, M. Abdul, et al. "A review of investigations on liquid fuel combustion in porous inert media." Progress in Energy and Combustion Science 35.2 (2009): 216-230.
[23]. Babkin, V. S. "Filtrational combustion of gases. Present state of affairs and prospects." Pure and Applied Chemistry 65.2 (1993): 335-344.
[24]. De Soete, G. "Stability and propagation of combustion waves in inert porous media." Symposium (International) on combustion. Vol. 11. No. 1. Elsevier, 1967.
[25]. Huang, Y., Christopher Yu Hang Chao, and P. Cheng. "Effects of preheating and operation conditions on combustion in a porous medium." International journal of heat and mass transfer 45.21 (2002): 4315-4324.
[26]. Zhdanok, S., Lawrence A. Kennedy, and G. Koester. "Superadiabatic combustion of methane air mixtures under filtration in a packed bed." Combustion and Flame 100.1-2 (1995): 221-231.
[27]. Zhdanok, S., Lawrence A. Kennedy, and G. Koester. "Superadiabatic combustion of methane air mixtures under filtration in a packed bed." Combustion and Flame 100.1-2 (1995): 221-231.
[28]. Mujeebu, M. Abdul, et al. "Combustion in porous media and its applications–A comprehensive survey." Journal of environmental management 90.8 (2009): 2287-2312.
[29]. Mujeebu, M. Abdul, et al. "Trends in modeling of porous media combustion." Progress in Energy and Combustion science 36.6 (2010): 627-650.
[30]. Janvekar, Ayub Ahmed, et al. "Effects of the preheat layer thickness on surface/submerged flame during porous media combustion of micro burner." Energy 122 (2017): 103-110.
[31]. Moffat, Robert J. "Using uncertainty analysis in the planning of an experiment." (1985): 173-178.